

PrefillShare: A Shared Prefill Module for KV Reuse in Multi-LLM Disaggregated Serving

Sunghyeon Woo,^{*} Hoseung Kim,^{*} Sunghwan Shim, Minjung Jo, Hyunjoon Jeong, Jeongtae Lee, Joonghoon Kim, Sungjae Lee, Baeseong Park, Se Jung Kwon, Dongsoo Lee

NAVER Cloud
 {sunghyeon.woo1, hoseung.kim}@navercorp.com

Abstract

Multi-agent systems increasingly orchestrate multiple specialized language models to solve complex real-world problems, often invoking them over a shared context. This execution pattern repeatedly processes the same prompt prefix across models. Consequently, each model redundantly executes the prefill stage and maintains its own key-value (KV) cache, increasing aggregate prefill load and worsening tail latency by intensifying prefill–decode interference in existing LLM serving stacks. Disaggregated serving reduces such interference by placing prefill and decode on separate GPUs, but disaggregation does not fundamentally eliminate inter-model redundancy in computation and KV storage for the same prompt. To address this issue, we propose PrefillShare, a novel algorithm that enables sharing the prefill stage across multiple models in a disaggregated setting. PrefillShare factorizes the model into prefill and decode modules, freezes the prefill module, and fine-tunes only the decode module. This design allows multiple task-specific models to share a prefill module and the KV cache generated for the same prompt. We further introduce a routing mechanism that enables effective prefill sharing across heterogeneous models in vLLM-based disaggregated system. PrefillShare not only matches full fine-tuning accuracy on a broad range of tasks and models, but also delivers $4.5\times$ lower p95 latency and $3.9\times$ higher throughput in multi-model agent workloads.

1. Introduction

Large language models (LLMs) have demonstrated superior performance across a wide range of tasks, including

reasoning, code generation, and knowledge-intensive question answering (Park et al., 2023; Chowdhery et al., 2023; Team et al., 2023; Achiam et al., 2023). Building on these advances, recent systems increasingly explore agentic workflows, where models interact with tools, intermediate memory states, and external resources to solve complex problems (Yao et al., 2022; Schick et al., 2023; Shinn et al., 2023). These developments highlight the growing role of LLMs as core components in interactive and multi-step systems. As part of this trend, some recent works propose agentic workflows that employ multiple specialized models to collaboratively solve a complex task, leveraging different models to specialize in distinct behaviors or capabilities (Shen et al., 2023; Hong et al., 2023; Wu et al., 2024; Su et al., 2025). Such multi-model approaches have been shown to improve task performance and modularity. However, this trend also introduces new challenges for efficient inference, particularly when workflows invoke multiple models over a shared context.

A key challenge arises from how autoregressive inference is executed in decoder-only Transformers. Modern serving systems (Kwon et al., 2023; Zheng et al., 2024) rely on KV caches to avoid recomputing attention over previously processed tokens. However, KV caches are tightly coupled to model parameters and cannot be reused across different models. Consequently, when multiple models process the same shared context, redundant prefill computation and duplicated KV caches become inevitable. This redundancy has two major implications. First, repeated prefill significantly increases latency by both raising time-to-first-token (TTFT) through additional prefill computation and worsening tail latency via intensified contention between prefill and decode in existing serving stacks (Zhong et al., 2024; Patel et al., 2024). Second, maintaining separate KV caches across models leads to rapid growth in memory consumption, limiting concurrency and complicating cache management in practical serving systems.

Disaggregated serving (Zhong et al., 2024; Patel et al., 2024) can alleviate the bottleneck in conventional serving stacks

^{*}Equal contribution .

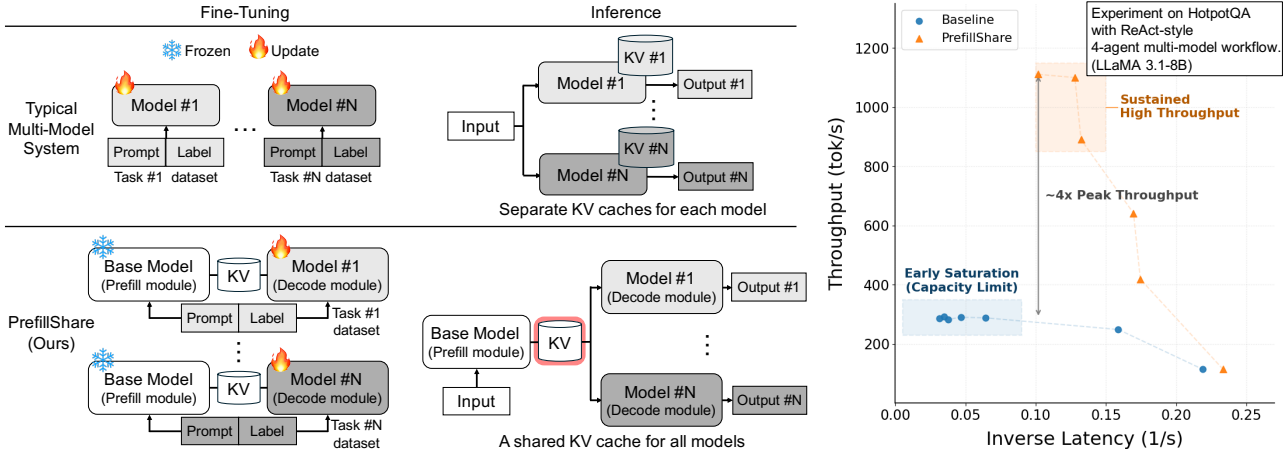


Figure 1. Comparison of a typical multi-model system and PrefillShare. (Left) In a typical multi-model system, each task-specific model is fine-tuned and served independently, maintaining its own KV cache for identical input prompts. PrefillShare decouples prefill and decoding into a shared prefill module and task-specific decode modules, fine-tuning only the decode modules, thereby enabling multiple task-specific decoders to reuse the same prompt KV cache. (Right) In a multi-model disaggregated serving (baseline), substantial computational overhead arises from redundant prefill on identical prompts and frequent recomputation due to explosive KV-cache growth and the resulting evictions under increasing load. PrefillShare shares KV caches across models to enable effective prefix caching and prevent early cache saturation, substantially reducing computation and achieving up to 4 \times higher throughput under high load.

by reducing contention between prefill and decode. By decoupling the compute-bound prefill phase from the memory-bound decoding phase and placing them on separate GPUs, disaggregated serving allows prefill capacity to scale without interfering with decoding. However, disaggregation alone does not fundamentally resolve cross-model redundancy. Even across differently fine-tuned models, identical prompts miss the opportunity to share prefill states and KV caches, leading to duplicated memory footprints and unnecessary system overhead.

Several recent works have explored approaches to fundamentally mitigate these inefficiencies. KVCOMM (Ye et al., 2025) explores cross-model communication to reuse KV information across overlapping contexts by aligning cache offsets using an online-maintained anchor pool in multi-agent settings. DroidSpeak (Liu et al., 2024) enables partial KV sharing across models by selectively reusing KV states from non-sensitive components, allowing reuse under specific architectural and sensitivity assumptions. While these approaches demonstrate the potential of cross-model reuse, additional coordination is often required, and robustness at broader scope is hard to guarantee without training for cross-model KV-cache sharing. ICaRus (Woo et al., 2026) decomposes a decoder-only Transformer into a frozen logical encoder and a trainable logical decoder, enabling identical KV reuse for the same prompt across fine-tuned models while maintaining robust accuracy. However, because the logical decoder in ICaRus is designed to consume only the KV cache produced by the logical encoder, the encoder must be executed alongside decoding, which introduces extra compute overhead and limits scalability under high

concurrency.

In this work, we propose PrefillShare, a shared-prefill disaggregated serving algorithm for multi-model agent workloads. Fig. 1 illustrates how PrefillShare decouples a shared prefill module from task-specific decoders, reusing the same prompt KV cache across models to avoid redundant prefill computation and duplicated KV storage. PrefillShare separates execution into two roles considering disaggregated inference scenario: a base prefill module that processes the shared context once to produce a KV cache, and multiple task-specific decode modules that generate outputs by consuming the shared cache. This design eliminates redundant prefill computation and avoids duplicating large KV caches across models when switching between specialized decoders. To make shared-prefill inference robust, we introduce a cache-conditioned fine-tuning procedure that freezes the prefill module and fine-tunes only the decode module to generate tokens conditioned on the base model’s KV cache. We further design an efficient routing and cache-handoff mechanism in a vLLM-based disaggregated system to support heterogeneous specialized models. Together, PrefillShare enables scalable multi-model serving while preserving the accuracy of full fine-tuning in various tasks and models, significantly reducing tail latency and improving throughput in multi-model agent workloads.

In summary, we make the following contributions:

- **Cross-model prefill and KV-cache sharing.** We propose PREFILLSHARE, a novel algorithm that enables multiple task-specific models to share the prefill stage

and the resulting KV cache for the same prompt in disaggregated serving, eliminating redundant prefill computation and duplicate KV-cache storage across models.

- **Cache-conditioned fine-tuning for robust sharing.** We introduce a disaggregation-aware training procedure that factorizes a model into prefill and decode modules, freezes the prefill module, and fine-tunes only the decode module conditioned on the shared KV cache, aligning training with the prefill-sharing inference setup while matching full fine-tuning accuracy.
- **Routing and cache-handoff mechanism for prefill sharing.** We design an efficient routing and cache-handoff mechanism in a vLLM-based heterogeneous disaggregated serving system to make shared-prefill inference practical, achieving up to **4.5**× lower p95 latency and up to **3.9**× higher throughput in multi-model agent workloads.

2. Background

2.1. Single Model Autoregressive Inference

Let $X = \{x_1, \dots, x_n\}$ be an input prompt of length n , and $Y = \{y_1, \dots, y_T\}$ be the generated output sequence of length T . An LLM parameterized by θ models the conditional likelihood of Y given X as:

$$P(Y|X) = \prod_{t=1}^T P(y_t|X, y_{<t}; \theta) \quad (1)$$

where $y_{<t}$ denotes the tokens generated prior to step t .

To efficiently compute these probabilities without redundant operations, inference systems maintain a KV cache. Let \mathbf{k}_t and \mathbf{v}_t denote the key and value tensors produced at decoding step t , aggregated across all layers. The KV cache state \mathcal{C}_t is defined as the concatenation of past keys and values:

$$\mathcal{C}_t = [\mathcal{C}_{t-1}; (\mathbf{k}_t, \mathbf{v}_t)] \quad (2)$$

where $[\cdot; \cdot]$ denotes the concatenation operation along the sequence length dimension. Note that the size of \mathcal{C}_t grows linearly with the sequence length.

Two-Phase Execution. We formalize the Transformer forward pass as a function $(y, \Delta\mathcal{C}) = \mathcal{F}_\theta(x, \mathcal{C}_{\text{past}})$, which takes the current input tokens x and the past cache $\mathcal{C}_{\text{past}}$, and returns the next token y and the incremental cache update $\Delta\mathcal{C}$. In practice, inference is executed in two phases:

Prefill Phase: The model processes the entire prompt X in parallel. Since there is no prior history, the cache is initialized as empty (\emptyset). The function computes the first output token y_1 and generates the full initial cache \mathcal{C}_n corresponding to the prompt:

$$(y_1, \mathcal{C}_n) = \mathcal{F}_\theta(X, \emptyset) \quad (3)$$

Decode Phase: For subsequent steps $t = 2 \dots T$, the model generates tokens autoregressively. At each step, it takes the previously generated token y_{t-1} and the current cache \mathcal{C}_{n+t-2} to produce the next token and the incremental cache update:

$$(y_t, \Delta\mathcal{C}_t) = \mathcal{F}_\theta(y_{t-1}, \mathcal{C}_{n+t-2}) \quad (4)$$

The cache is updated as $\mathcal{C}_{n+t-1} = [\mathcal{C}_{n+t-2}; \Delta\mathcal{C}_t]$. This decode phase is typically memory-bound, as it repeatedly loads and extends a large cache state.

2.2. Multi-Model Inference and Prefix Caching

Recent advancements in agentic workflows have led to the deployment of multi-model systems, where a set of N specialized models $\{\mathcal{M}_1, \dots, \mathcal{M}_N\}$ collaborate to solve complex tasks. In these scenarios, different models frequently process the same shared context X (e.g., a long conversation history, a common system prompt, or a shared document) to generate diverse responses.

To mitigate the high computational cost of the prefill phase, modern serving systems (Kwon et al., 2023) cache the prefix KV caches for frequently occurring prompt prefixes. For an incoming request with input X , the system checks whether the KV cache for any prefix of X already exists in a pool of cached blocks. If a match is found, the system reuses the cached KV blocks and skips the redundant prefill computation for the matched prefix, effectively turning expensive prefill into a lightweight memory lookup and substantially reducing latency.

However, prefix caching does not directly extend to multi-model settings because KV caches are tightly coupled to model parameters. Even when the input prompt X is identical, two models \mathcal{M}_i and \mathcal{M}_j with $\theta_i \neq \theta_j$ produce different key and value representations at each layer, resulting in incompatible cache states. As a result, KV caches computed by one model are generally incompatible with other models and cannot be reused across models. Therefore, multi-model workflows must recompute the prefill phase and maintain separate KV caches for each model, causing both redundant computation and duplicated memory footprints.

2.3. Disaggregated Serving

Modern LLM serving systems typically employ continuous batching (Yu et al., 2022; Kwon et al., 2023) to maximize

throughput by dynamically interleaving prefill and decode execution within the same scheduling loop. While this improves GPU utilization, it introduces interference between requests. To incorporate a new prefill request into an active batch, the system must execute the prefill phase, which preempts the ongoing decode phase and delays token generation for existing requests. As a result, ongoing generation may stall until the prefill computation completes, leading to unpredictable spikes in inter-token latency (ITL) and degrading interactive responsiveness (Agrawal et al., 2023).

To resolve this issue, recent works propose disaggregated serving (Zhong et al., 2024; Patel et al., 2024; Feng et al., 2025), which physically decouples the infrastructure into dedicated prefill and decode instances. By isolating prefill execution from the decode loop, disaggregated serving prevents prefill computation from interfering with autoregressive decoding, providing more stable ITL in real-world deployments.

3. Method

In this section, we present PrefillShare, including a disaggregated serving formulation with a shared prefill module and a cache-conditioned fine-tuning procedure that ensures cache compatibility between the base and specialized models.

3.1. Definitions and Formulation

Building on the autoregressive formulation in Section 2, we define two operational roles for inference: a prefill module that produces a shared KV cache from the input prompt and a decode module that generates task-specific outputs by consuming the shared cache.

Base Prefill Module. Let the base prefill module be a foundation model $\mathcal{M}_{\text{base}}$ with parameters θ_{base} . θ_{base} is responsible only for the prefill phase. It processes the input X once to produce a shared KV cache $\mathcal{C}_{\text{base}}$

$$(\cdot, \mathcal{C}_{\text{base}}) = \mathcal{F}_{\theta_{\text{base}}}(X, \emptyset) \quad (5)$$

Here $\mathcal{C}_{\text{base}}$ denotes the shared KV cache. Note that $\mathcal{M}_{\text{base}}$ computes the KV cache but does not participate in the subsequent token generation loop.

Specialized Decode Module. For each task, we construct a decode module \mathcal{M}_{dec} with parameters θ_{dec} . At inference time, the decode module initializes its cache with $\mathcal{C} \leftarrow \mathcal{C}_{\text{base}}$ and generates the output sequence:

$$(y_t, \Delta \mathcal{C}_t) = \mathcal{F}_{\theta_{\text{dec}}}(y_{t-1}, \mathcal{C}) \quad (6)$$

This separation enables multiple decode modules to reuse

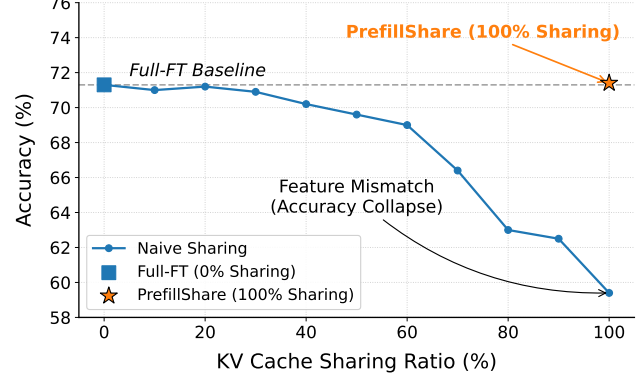


Figure 2. GSM8K accuracy as a function of KV cache sharing ratio between the base and fine-tuned models. Naive sharing without cache-adaptive fine-tuning collapses at high sharing ratios, while PrefillShare preserves near Full-FT accuracy even at 100% sharing.

the same shared prefill cache while preserving task-specific generation behavior.

3.2. Cache-Conditioned Fine-Tuning

A key challenge in PrefillShare is that the decode module must generate tokens while attending to a KV cache produced by a different parameterization. In standard fine-tuning, the model implicitly learns to decode from its self-generated cache, since both prefill and decoding are produced by the same parameters. As a result, the learned KV representations become tightly coupled to the model parameters. When the decode model reuses an increasing fraction of KV caches produced by a different model, accuracy degrades and eventually collapses, as shown in Fig. 2.

PrefillShare aims to enable a task-specific decode module \mathcal{M}_{dec} to generate tokens by conditioning on a shared prompt cache $\mathcal{C}_{\text{base}}$ computed by a frozen base prefill module $\mathcal{M}_{\text{base}}$. This setting requires \mathcal{M}_{dec} to reliably decode from $\mathcal{C}_{\text{base}}$, even though the KV representations in $\mathcal{C}_{\text{base}}$ differ from those that would be produced under the task-specific parameters θ_{dec} .

To address this mismatch and enable robust shared-prefill inference, we propose cache-conditioned fine-tuning, a disaggregation-aware training procedure that explicitly trains the decode module to consume $\mathcal{C}_{\text{base}}$. For each training example (X, Y) , we first compute the shared cache $\mathcal{C}_{\text{base}}$ using $\mathcal{M}_{\text{base}}$ from input prompt X , and treat the cache as a constant input so that gradients do not propagate into θ_{base} . We then fine-tune only the task-specific decode module \mathcal{M}_{dec} with parameters θ_{dec} to predict the target sequence while conditioning on the base cache:

$$\mathcal{L}(\theta_{\text{dec}}) = - \sum_t \log P(y_t \mid y_{t-1}, \mathcal{C}_{\text{base}}; \theta_{\text{dec}}) \quad (7)$$

We train \mathcal{M}_{dec} with teacher forcing, feeding the ground-truth prefix $y_{<t}$ while conditioning on the fixed cache $\mathcal{C}_{\text{base}}$. Notably, cache-conditioned fine-tuning preserves the standard next-token prediction objective, but replaces the self-generated cache with the shared base cache as the conditioning signal.

By optimizing (7), the decode module learns to align its attention features and token generation behavior with the KV cache distribution produced by $\mathcal{M}_{\text{base}}$. In other words, cache-conditioned fine-tuning enables the decode module \mathcal{M}_{dec} to effectively interpret the base KV cache $\mathcal{C}_{\text{base}}$ produced by $\mathcal{M}_{\text{base}}$, whereas naive KV-cache sharing can substantially degrade accuracy due to KV representations mismatch, as shown in Fig. 2. Consequently, this alignment enables reliable reuse of the shared base cache across heterogeneous task-specific decode modules without requiring parameter synchronization between the base and fine-tuned models. Furthermore, this training procedure matches the inference-time cache usage, improving reliability under shared-prefill serving.

3.3. Disaggregated Inference Workflow

We leverage the cache-compatible nature of PrefillShare to build an efficient disaggregated execution pipeline for multi-model agent workloads, where a single user request is processed by multiple specialized decoders in sequence. In such workflows, the system frequently switches between heterogeneous models (e.g., Planner \rightarrow Coder \rightarrow Reviewer) while operating over a largely shared session context. Current disaggregated serving still incurs repeated prefill computation at every model switch, since each model must reconstruct its own KV cache even for identical prefixes. PrefillShare removes this structural redundancy by reusing a shared prefill cache across model transitions, making the benefit more pronounced as the shared context grows and the number of invoked modules increases.

Prefix-Aware Routing. A practical challenge in multi-model serving is preserving prefix-cache locality as requests are forwarded between multiple decode models over a shared context. To maximize cache reuse, PrefillShare employs a prefix-locality-aware routing policy that keeps requests with the same shared prefix pinned to a consistent prefill worker whenever possible, enabling incremental cache extension instead of recomputing the prefix from scratch.

Execution Pipeline. PrefillShare executes a multi-model request as an alternating sequence of prefill and decode steps over a shared context. Let $X^{(0)}$ denote the initial prompt, and let $X^{(i)} = [X^{(i-1)}; Y^{(i)}]$ be the context after the i -th specialized model generates an output segment $Y^{(i)}$. The pipeline repeatedly performs the following operations:

1. **Shared / Partial Prefill:** a prefill worker produces the shared cache $\mathcal{C}_{\text{base}}^{(i)}$ for the current context $X^{(i)}$. The first step processes the full initial prompt, while later steps perform partial prefill to extend the cache only for newly appended tokens.
2. **Selective Decode:** a selected specialized decode module consumes $\mathcal{C}_{\text{base}}^{(i)}$ to generate $Y^{(i)}$. Since decoding starts from the shared cache, switching across heterogeneous decoders does not require recomputing the shared prefix.
3. **Cache Handoff:** the shared cache is transferred to the next decode stage, and the generated tokens are appended to the context for the next partial prefill step.

By iterating these steps, PrefillShare supports practical multi-model workflows where a single user request triggers multiple specialized decoders over a shared context, while the shared prefix cache is computed once and incrementally extended across model switches.

Efficiency Analysis. We quantify the memory complexity by decomposing the sequence into a shared prefix L_{shared} and a model-specific segment L_{unique} . In the baseline setup, each model maintains its own KV cache for the full sequence, so the memory requirement scales linearly with the number of models:

$$\text{Mem}_{\text{baseline}} = O(N \cdot (L_{\text{shared}} + L_{\text{unique}})). \quad (8)$$

In contrast, PrefillShare stores the shared prefix cache once and maintains only model-specific cache segments per decode module:

$$\text{Mem}_{\text{PrefillShare}} = O(L_{\text{shared}} + N \cdot L_{\text{unique}}). \quad (9)$$

In multi-model workflows, when $L_{\text{shared}} \gg L_{\text{unique}}$, this changes the dominant term from $N \cdot L_{\text{unique}}$ to L_{shared} , making the primary memory cost effectively independent of the number of decode modules N . This structural efficiency also improves responsiveness when switching between specialized modules. In typical serving, invoking a new model \mathcal{M}_k typically requires re-running the prefill phase over the shared context, which increases TTFT as the context grows. PrefillShare avoids this compute overhead by reusing $\mathcal{C}_{\text{base}}$, so TTFT becomes largely insensitive to L_{shared} .

4. Experiments

4.1. Experimental Setup

Training Setup We evaluate PrefillShare across multiple datasets and model sizes. We compare full fine-

Table 1. Accuracy on math, coding, and tool-calling benchmarks for LLaMA3.1-8B and Qwen3-8B-Base after full fine-tuning (Full-FT) or cache-conditioned fine-tuning (reported as PrefillShare). For each domain, models are fine-tuned on MetaMathQA-40K (math), EvolInstruct-Code-80K (coding), and xLAM-function-calling-60K (tool calling), and evaluated on GSM8K/GSM+, HumanEval/HumanEval+, and BFCL (Simple Python/Multiple), respectively. PrefillShare achieves accuracy comparable to full fine-tuned models across all evaluated benchmarks.

Configuration	KV Sharing	Math		Coding		Tool calling	
		GSM8K	GSM+	HumanEval	HumanEval+	Simple Python	Multiple
LLaMA3.1-8B	Inherent	25.9	18.0	36.6	29.9	70.5	45.5
Full-FT	Not Supported	71.3	49.8	48.2	45.7	90.0	88.0
PrefillShare (Ours)	Supported	71.4	49.3	48.8	45.1	90.7	88.5
Qwen3-8B-Base	Inherent	11.8	12.5	68.3	61.6	81.5	80.0
Full-FT	Not Supported	85.8	65.7	83.5	74.3	93.3	92.0
PrefillShare (Ours)	Supported	84.8	64.5	86.6	80.5	93.5	91.0

Table 2. Accuracy of Full-FT and PrefillShare on GSM8K and GSM+ across model sizes fine-tuned on MetaMathQA-40K. Q3-1.7B/8B/14B-Base represents Qwen3-1.7B/8B/14B, respectively. PrefillShare maintains comparable accuracy over full fine-tuning across all evaluated model sizes, indicating robustness to model scale.

Configuration	Q3-1.7B-Base		Q3-8B-Base		Q3-14B-Base	
	GSM8K	GSM+	GSM8K	GSM+	GSM8K	GSM+
Full-FT	75.0	54.8	85.8	65.7	88.1	67.5
PrefillShare	75.4	53.9	84.8	64.5	88.1	66.7

tuning (Full-FT) with cache-conditioned fine-tuning (PrefillShare) on LLaMA3.1-8B (Grattafiori et al., 2024) and Qwen3-1.7B/8B/14B-Base (Yang et al., 2025). For domain-specific adaptation, we fine-tune separate models on MetaMathQA-40K (Yu et al., 2023) (math), EvolInstruct-Code-80K (Luo et al., 2023) (coding), and xLAM-function-calling-60K (Zhang et al., 2025) (tool calling). Each domain-specific model is evaluated on its corresponding benchmark: GSM8K/GSM+ (Cobbe et al., 2021; Li et al., 2024) for math, HumanEval/HumanEval+ (Chen, 2021; Liu et al., 2023) for coding, and the Berkeley Function Calling Leaderboard (BFCL) (Patil et al., 2025) for tool calling using the Simple Python and Multiple subsets. Detailed training setup can be found in Appendix A.

Inference Setup We evaluate PrefillShare in a multi-model agent serving scenario where each session runs a four-agent, multi-turn workflow; in each turn, all agents are invoked sequentially over a largely shared prefix, inducing frequent model switching. We instantiate representative agentic prompting patterns such as ReAct and Reflexion, following experimental setups in prior LLM agent and serving studies (Kim et al., 2025; Woo et al., 2026).

We compare against a disaggregated serving baseline that deploys independent prefill/decode pipelines per model. In

the baseline, each model is served by a dedicated prefill GPU and a dedicated decode GPU, resulting in four isolated prefill/decode pairs (8 GPUs total). PrefillShare uses the same total GPU budget (4 prefill GPUs and 4 decode GPUs), but shares prefill across all decoders via cross-model KV-cache reuse. All experiments use LLaMA-3.1-8B on a single A100 node, implemented by extending vLLM’s disaggregated serving pipeline. Additional implementation details are provided in Appendix B.1

4.2. Training and Accuracy Evaluation

Robust accuracy in various tasks. Table 1 demonstrates that PrefillShare achieves accuracy comparable to conventional Full-FT across math, coding, and tool calling, even outperforming Full-FT in several cases. Specifically, PrefillShare attains accuracy within 1% of Full-FT across all tasks, while achieving higher accuracy on GSM8K, HumanEval, and the tool-calling benchmark. We observe a similar trend on Qwen3-8B-Base, where PrefillShare remains competitive on most tasks and yields substantial improvements on coding tasks. We attribute this robust accuracy in PrefillShare to cache-conditioned fine-tuning, which enables the model to interpret KV representations produced by a frozen, shared prefill module. Moreover, updating only the decode module can be interpreted as a form of strict regularization, which may explain the superior performance of PrefillShare over conventional fine-tuning on certain tasks.

Scaleup to model sizes. We next examine how PrefillShare scales with model size using Qwen3-1.7B/8B/14B-Base under the math fine-tuning scenario (Table 2). Across all three model sizes, PrefillShare achieves GSM8K/GSM+ accuracy comparable to Full-FT, indicating that cache-conditioned fine-tuning remains effective from smaller (1.7B) to larger (14B) backbones. Overall, these results suggest that PrefillShare exhibits limited sensitivity to model scale and can be applied consistently across deployments

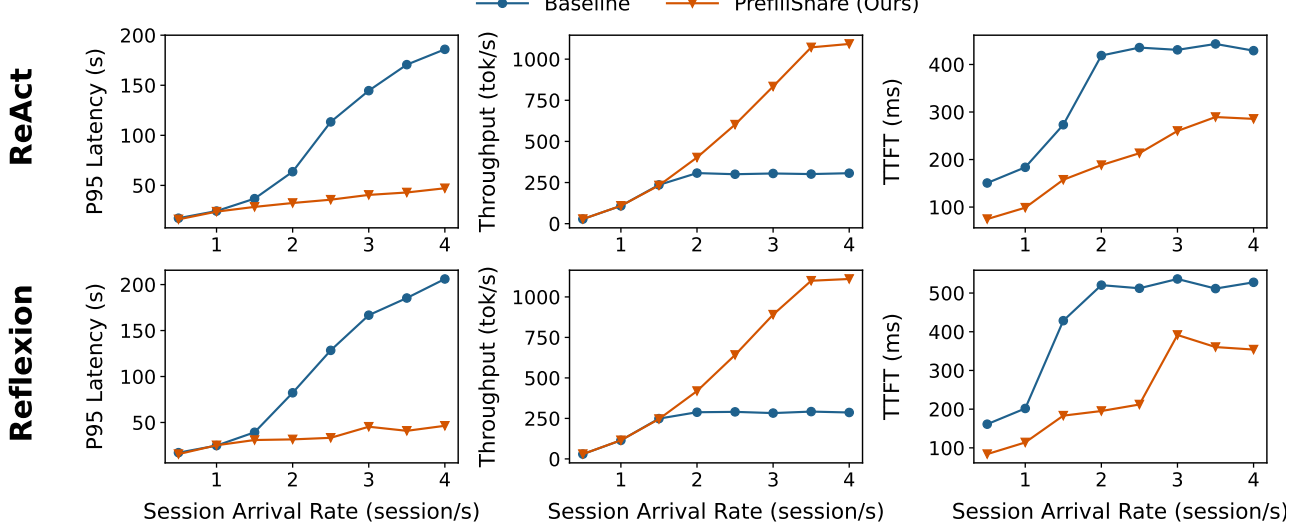


Figure 3. Serving performance under multi-model agent workloads. We compare the disaggregated baseline and PrefillShare under increasing session arrival rates for two representative agentic patterns: ReAct (top) and Reflexion (bottom). We report p95 end-to-end latency, throughput, and TTFT. PrefillShare outperforms the baseline in both patterns, with the gap widening as the session arrival rate increases, primarily due to rising prefix-cache miss rates in the baseline.

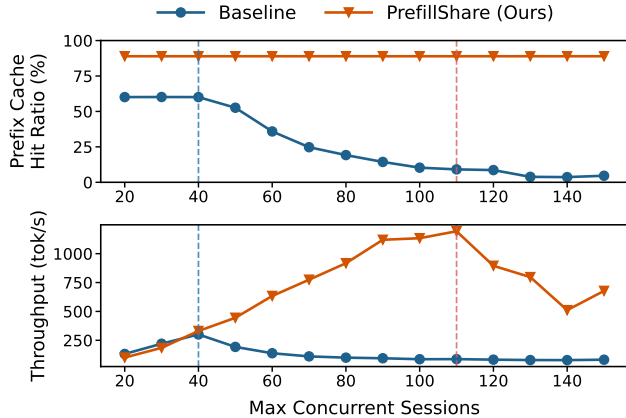


Figure 4. Prefix cache hit ratio and throughput under varying max concurrent sessions. Top: prefix cache hit ratio (%). Bottom: throughput (tok/s). The baseline degrades beyond ≈ 40 sessions as reduced prefix reuse lowers both metrics, whereas PrefillShare sustains higher throughput over a wider range, with high-concurrency saturation driven by handoff overheads.

with varying model sizes without sacrificing accuracy.

4.3. Serving Performance under Multi-Model Agent Workloads

End-to-end serving performance under multi-model agent workloads. Fig. 3 compares the serving performance of PrefillShare against the disaggregated baseline under increasing session arrival rates, reporting p95 end-to-end latency, throughput, and TTFT for both ReAct and

Reflexion workloads. At low load, both systems achieve similar latency and throughput. As the arrival rate increases, however, the baseline experiences rapidly growing tail latency and diminished throughput due to redundant prefill work and duplicated prefix KV management across model switches.

In contrast, PrefillShare amortizes shared-prefix processing across decoders, sustaining higher throughput while keeping tail latency low. Overall, PrefillShare achieves up to 3.9 \times lower p95 latency and 3.6 \times higher throughput on ReAct, and up to 4.5 \times lower p95 latency and 3.9 \times higher throughput on Reflexion, demonstrating substantially improved scalability under high offered load.

Impact of max concurrent sessions on prefix cache reuse and throughput. Fig. 4 examines the effect of the max concurrent sessions, which caps the number of active sessions admitted to the system. This knob is important in practice not only for preventing overload and out-of-memory, but also because it directly controls the system-wide KV footprint. As concurrency increases, serving systems must retain more prefix KV cache per active session, which increases memory pressure and can trigger more frequent cache eviction. This reduces the prefix cache hit ratio and leads to additional prefill recomputation. In the disaggregated baseline, this effect is amplified because each model maintains its own prefix KV cache for the same session context, rapidly multiplying the total KV footprint.

For the results in Fig. 3, we therefore sweep the concur-

rency limit and report the best-performing configuration for each setting. In Fig. 4, we fix the session arrival rate to 4 sessions/s under the ReAct workload and vary the max concurrent sessions. The baseline shows a clear degradation beyond around 40 concurrent sessions, where the prefix cache hit ratio peaks at 60% before dropping sharply, causing throughput to decrease accordingly.

PrefillShare exhibits a different scaling behavior. Unlike the baseline, the prefix cache hit ratio stays consistently high at nearly 89% across concurrency levels, reflecting the elimination of duplicated prefix KV storage through shared prefill. Throughput continues to increase with concurrency as prefill sharing reduces redundant KV storage and computation, improving effective GPU utilization. Notably, around 110 concurrent sessions, throughput begins to saturate and eventually decline even though the prefix cache hit ratio remains largely unchanged, indicating that the performance drop is not driven by reduced prefix reuse. At higher concurrency, decode-side KV pressure increases handoff overhead (e.g., KV staging/reload in our vLLM prototype; Appendix B.2), which eventually dominates and reduces the effective throughput. Overall, PrefillShare sustains higher throughput over a wider concurrency range by maintaining stable prefix reuse, and the remaining throughput drop at extreme concurrency is driven by handoff-related pressure rather than prefix cache inefficiency. We observe the same qualitative trends with Qwen3-14B under identical workloads and system settings; additional results are provided in Appendix B.3.

5. Related Work

Efficient LLM Serving and KV Management. The rapid growth of large language models has motivated extensive research on efficient inference and serving systems, particularly to address the substantial memory footprint of KV caches. FlashAttention (Dao et al., 2022; Dao, 2023) fuses attention operations to avoid materializing intermediate states, cutting memory-bandwidth overhead. PageDAttention (Kwon et al., 2023) organizes KV caches into fixed-size blocks to reduce fragmentation and enable larger effective batch sizes.

In addition to optimizing how KV caches are stored and allocated, recent systems reduce KV overhead by reusing previously computed caches across requests. Prefix caching reuses KV states for frequently occurring input prefixes (Gim et al., 2024; Pan et al., 2025), reducing redundant prefill in workloads such as those with repeated prompts, templated inputs, or multi-turn interactions. SGLang (Zheng et al., 2024) introduces RadixAttention, which organizes KV caches in a radix-tree structure to efficiently support prefix-level reuse across requests.

Disaggregated Serving. Modern LLM serving systems use continuous batching to interleave prefill and decode for high throughput, but long and compute-intensive prefill operations can stall latency-sensitive decoding, causing unstable inter-token latency.

To address this problem, several works propose disaggregated serving architectures that explicitly separate prefill and decode execution. DistServe (Zhong et al., 2024) decouples these phases onto dedicated resources, ensuring that decoding is not blocked by incoming prefill requests and significantly improving latency stability under high load. Similarly, Splitwise (Patel et al., 2024) formalizes phase splitting as a system-level optimization, demonstrating improved goodput by isolating the distinct computational characteristics of prefill and decode. In addition to phase separation, recent systems explore KV cache-centric designs that decouple cache management from execution, such as Mooncake (Qin et al., 2024), and KV cache connector frameworks such as LMCache (Liu et al., 2025), further highlighting the importance of disaggregation in large-scale serving systems.

Multi-Model and Agentic Inference. Agentic AI enables complex task solving via structured reasoning, planning, and tool interaction (Yao et al., 2022; Schick et al., 2023; Shinn et al., 2023; Wei et al., 2022; Wang et al., 2023). Building on this, multi-agent frameworks such as LangChain (Team, 2023) and AutoGen (Wu et al., 2024) assign specialized roles and structured communication to improve modularity and performance on multi-step tasks.

Recent work shows that smaller language models, while efficient, struggle to robustly learn multi-step tool usage, motivating workflows that combine models with complementary capabilities (Chen et al., 2023; Shen et al., 2024; Wang et al., 2024). Similarly, systems such as ToolOrchestra (Su et al., 2025) explicitly orchestrate multiple models and tools to leverage their respective strengths, reinforcing the need for heterogeneous, multi-model execution in practical agentic settings.

From a systems perspective, multi-model agentic workflows introduce additional challenges. When models independently process shared context, serving systems incur redundant prefill and duplicated KV caches. Several recent works address this inefficiency, including DroidSpeak (Liu et al., 2024) and KVComm (Ye et al., 2025), which explore limited forms of cross-model reuse through partial state sharing or inter-model communication.

6. Conclusion

We proposed PrefillShare, a disaggregated serving algorithm that eliminates redundant prefill computation and duplicated KV caches in multi-model LLM workloads by separating

inference into a shared prefill module and task-specific decode modules, thereby enabling cross-model reuse of prefill computation. Enabled by cache-conditioned fine-tuning, which aligns specialized decoders with a frozen shared prefill module, our approach preserves task accuracy while substantially improving serving efficiency across diverse tasks, model scales, and realistic multi-model agent workloads, achieving significantly lower tail latency and higher throughput. These results suggest that shared-prefill execution is a promising foundation for scalable multi-model and agentic LLM serving.

References

Achiam, J., Adler, S., Agarwal, S., Ahmad, L., Akkaya, I., Aleman, F. L., Almeida, D., Altenschmidt, J., Altman, S., Anadkat, S., et al. Gpt-4 technical report. *arXiv preprint arXiv:2303.08774*, 2023.

Agrawal, A., Panwar, A., Mohan, J., Kwatra, N., Gulavani, B. S., and Ramjee, R. Sarathi: Efficient llm inference by piggybacking decodes with chunked prefills. *arXiv preprint arXiv:2308.16369*, 2023.

Chen, L., Zaharia, M., and Zou, J. Frugalgpt: How to use large language models while reducing cost and improving performance. *arXiv preprint arXiv:2305.05176*, 2023.

Chen, M. Evaluating large language models trained on code. *arXiv preprint arXiv:2107.03374*, 2021.

Chowdhery, A., Narang, S., Devlin, J., Bosma, M., Mishra, G., Roberts, A., Barham, P., Chung, H. W., Sutton, C., Gehrmann, S., et al. Palm: Scaling language modeling with pathways. *Journal of Machine Learning Research*, 24(240):1–113, 2023.

Cobbe, K., Kosaraju, V., Bavarian, M., Chen, M., Jun, H., Kaiser, L., Plappert, M., Tworek, J., Hilton, J., Nakano, R., et al. Training verifiers to solve math word problems. *arXiv preprint arXiv:2110.14168*, 2021.

Dao, T. Flashattention-2: Faster attention with better parallelism and work partitioning. *arXiv preprint arXiv:2307.08691*, 2023.

Dao, T., Fu, D., Ermon, S., Rudra, A., and Ré, C. Flashattention: Fast and memory-efficient exact attention with io-awareness. *Advances in neural information processing systems*, 35:16344–16359, 2022.

Diao, S., Pan, R., Dong, H., Shum, K. S., Zhang, J., Xiong, W., and Zhang, T. Lmflow: An extensible toolkit for finetuning and inference of large foundation models, 2024. URL <https://arxiv.org/abs/2306.12420>.

Feng, J., Huang, Y., Zhang, R., Liang, S., Yan, M., and Wu, J. Windserve: Efficient phase-disaggregated llm serving with stream-based dynamic scheduling. In *Proceedings of the 52nd Annual International Symposium on Computer Architecture*, pp. 1283–1295, 2025.

Gim, I., Chen, G., Lee, S.-s., Sarda, N., Khandelwal, A., and Zhong, L. Prompt cache: Modular attention reuse for low-latency inference. *Proceedings of Machine Learning and Systems*, 6:325–338, 2024.

Grattafiori, A., Dubey, A., Jauhri, A., Pandey, A., Kadian, A., Al-Dahle, A., Letman, A., Mathur, A., Schelten, A., Vaughan, A., et al. The llama 3 herd of models. *arXiv preprint arXiv:2407.21783*, 2024.

Hong, S., Zhuge, M., Chen, J., Zheng, X., Cheng, Y., Wang, J., Zhang, C., Wang, Z., Yau, S. K. S., Lin, Z., et al. Metagpt: Meta programming for a multi-agent collaborative framework. In *The Twelfth International Conference on Learning Representations*, 2023.

Kim, J., Shin, B., Chung, J., and Rhu, M. The cost of dynamic reasoning: Demystifying ai agents and test-time scaling from an ai infrastructure perspective. *arXiv preprint arXiv:2506.04301*, 2025.

Kwon, W., Li, Z., Zhuang, S., Sheng, Y., Zheng, L., Yu, C. H., Gonzalez, J., Zhang, H., and Stoica, I. Efficient memory management for large language model serving with pagedattention. In *Proceedings of the 29th symposium on operating systems principles*, pp. 611–626, 2023.

Langley, P. Crafting papers on machine learning. In Langley, P. (ed.), *Proceedings of the 17th International Conference on Machine Learning (ICML 2000)*, pp. 1207–1216, Stanford, CA, 2000. Morgan Kaufmann.

Li, Q., Cui, L., Zhao, X., Kong, L., and Bi, W. Gsm-plus: A comprehensive benchmark for evaluating the robustness of llms as mathematical problem solvers. *arXiv preprint arXiv:2402.19255*, 2024.

Liu, J., Xia, C. S., Wang, Y., and Zhang, L. Is your code generated by chatgpt really correct? rigorous evaluation of large language models for code generation. *Advances in Neural Information Processing Systems*, 36:21558–21572, 2023.

Liu, Y., Huang, Y., Yao, J., Feng, S., Gu, Z., Du, K., Li, H., Cheng, Y., Jiang, J., Lu, S., et al. Droidspeak: Kv cache sharing for cross-llm communication and multi-llm serving. *arXiv preprint arXiv:2411.02820*, 2024.

Liu, Y., Cheng, Y., Yao, J., An, Y., Chen, X., Feng, S., Huang, Y., Shen, S., Zhang, R., Du, K., et al. Lmcache: An efficient kv cache layer for enterprise-scale llm inference. *arXiv preprint arXiv:2510.09665*, 2025.

Loshchilov, I. and Hutter, F. Decoupled weight decay regularization. *arXiv preprint arXiv:1711.05101*, 2017.

Luo, Z., Xu, C., Zhao, P., Sun, Q., Geng, X., Hu, W., Tao, C., Ma, J., Lin, Q., and Jiang, D. Wizardcoder: Empowering code large language models with evol-instruct. *arXiv preprint arXiv:2306.08568*, 2023.

Pan, Z., Patel, A., Hu, Z., Shen, Y., Guan, Y., Li, W.-L., Qin, L., Wang, Y., and Ding, Y. Kvflow: Efficient prefix caching for accelerating llm-based multi-agent workflows. *arXiv preprint arXiv:2507.07400*, 2025.

Park, J. S., O'Brien, J., Cai, C. J., Morris, M. R., Liang, P., and Bernstein, M. S. Generative agents: Interactive simulacra of human behavior. In *Proceedings of the 36th annual acm symposium on user interface software and technology*, pp. 1–22, 2023.

Pascanu, R., Mikolov, T., and Bengio, Y. On the difficulty of training recurrent neural networks. In *International conference on machine learning*, pp. 1310–1318. Pmlr, 2013.

Patel, P., Choukse, E., Zhang, C., Shah, A., Goiri, I., Maleki, S., and Bianchini, R. Splitwise: Efficient generative llm inference using phase splitting. In *2024 ACM/IEEE 51st Annual International Symposium on Computer Architecture (ISCA)*, pp. 118–132. IEEE, 2024.

Patil, S. G., Mao, H., Yan, F., Ji, C. C.-J., Suresh, V., Stoica, I., and Gonzalez, J. E. The berkeley function calling leaderboard (bfcl): From tool use to agentic evaluation of large language models. In *Forty-second International Conference on Machine Learning*, 2025.

Qin, R., Li, Z., He, W., Cui, J., Tang, H., Ren, F., Ma, T., Cai, S., Zhang, Y., Zhang, M., et al. Mooncake: A kvcache-centric disaggregated architecture for llm serving. *ACM Transactions on Storage*, 2024.

Schick, T., Dwivedi-Yu, J., Dessì, R., Raileanu, R., Lomeli, M., Hambro, E., Zettlemoyer, L., Cancedda, N., and Scialom, T. Toolformer: Language models can teach themselves to use tools. *Advances in Neural Information Processing Systems*, 36:68539–68551, 2023.

Shen, W., Li, C., Chen, H., Yan, M., Quan, X., Chen, H., Zhang, J., and Huang, F. Small llms are weak tool learners: A multi-llm agent. *arXiv preprint arXiv:2401.07324*, 2024.

Shen, Y., Song, K., Tan, X., Li, D., Lu, W., and Zhuang, Y. Hugginggpt: Solving ai tasks with chatgpt and its friends in hugging face. *Advances in Neural Information Processing Systems*, 36:38154–38180, 2023.

Shinn, N., Cassano, F., Gopinath, A., Narasimhan, K., and Yao, S. Reflexion: Language agents with verbal reinforcement learning. *Advances in Neural Information Processing Systems*, 36:8634–8652, 2023.

Srivastava, N., Hinton, G., Krizhevsky, A., Sutskever, I., and Salakhutdinov, R. Dropout: a simple way to prevent neural networks from overfitting. *The journal of machine learning research*, 15(1):1929–1958, 2014.

Su, H., Diao, S., Lu, X., Liu, M., Xu, J., Dong, X., Fu, Y., Belcak, P., Ye, H., Yin, H., et al. Toolorchestra: Elevating intelligence via efficient model and tool orchestration. *arXiv preprint arXiv:2511.21689*, 2025.

Team, G., Anil, R., Borgeaud, S., Alayrac, J.-B., Yu, J., Soricut, R., Schalkwyk, J., Dai, A. M., Hauth, A., Millican, K., et al. Gemini: a family of highly capable multimodal models. *arXiv preprint arXiv:2312.11805*, 2023.

Team, L. Langchain: Building applications with large language models. <https://github.com/langchain-ai/langchain>, 2023. Accessed: 2025-01.

Wang, J., Wang, J., Athiwaratkun, B., Zhang, C., and Zou, J. Mixture-of-agents enhances large language model capabilities. *arXiv preprint arXiv:2406.04692*, 2024.

Wang, L., Xu, W., Lan, Y., Hu, Z., Lan, Y., Lee, R. K.-W., and Lim, E.-P. Plan-and-solve prompting: Improving zero-shot chain-of-thought reasoning by large language models. *arXiv preprint arXiv:2305.04091*, 2023.

Wei, J., Wang, X., Schuurmans, D., Bosma, M., Ichter, B., Xia, F., Chi, E., Le, Q., and Zhou, D. Chain-of-thought prompting elicits reasoning in large language models. In *Advances in Neural Information Processing Systems (NeurIPS)*, volume 35, pp. 24824–24837, 2022.

Woo, S., Kil, J., Kim, H., Kim, M., Kim, J., Seo, A., Lee, S., Jo, M., Ryu, J., Park, B., Kwon, S. J., and Lee, D. Icarus: Identical cache reuse for efficient multi-model inference. In *International Conference on Learning Representations (ICLR)*, 2026.

Wu, Q., Bansal, G., Zhang, J., Wu, Y., Li, B., Zhu, E., Jiang, L., Zhang, X., Zhang, S., Liu, J., et al. Autogen: Enabling next-gen llm applications via multi-agent conversations. In *First Conference on Language Modeling*, 2024.

Yang, A., Li, A., Yang, B., Zhang, B., Hui, B., Zheng, B., Yu, B., Gao, C., Huang, C., Lv, C., et al. Qwen3 technical report. *arXiv preprint arXiv:2505.09388*, 2025.

Yao, S., Zhao, J., Yu, D., Du, N., Shafran, I., Narasimhan, K. R., and Cao, Y. React: Synergizing reasoning and acting in language models. In *The eleventh international conference on learning representations*, 2022.

Ye, H., Gao, Z., Ma, M., Wang, Q., Fu, Y., Chung, M.-Y., Lin, Y., Liu, Z., Zhang, J., Zhuo, D., et al. Kvcomm: Online cross-context kv-cache communication for efficient llm-based multi-agent systems. *arXiv preprint arXiv:2510.12872*, 2025.

Yu, G.-I., Jeong, J. S., Kim, G.-W., Kim, S., and Chun, B.-G. Orca: A distributed serving system for {Transformer-Based} generative models. In *16th USENIX Symposium on Operating Systems Design and Implementation (OSDI 22)*, pp. 521–538, 2022.

Yu, L., Jiang, W., Shi, H., Yu, J., Liu, Z., Zhang, Y., Kwok, J. T., Li, Z., Weller, A., and Liu, W. Metamath: Bootstrap your own mathematical questions for large language models. *arXiv preprint arXiv:2309.12284*, 2023.

Zhang, J., Lan, T., Zhu, M., Liu, Z., Hoang, T. Q., Kokane, S., Yao, W., Tan, J., Prabhakar, A., Chen, H., et al. xlam: A family of large action models to empower ai agent systems. In *Proceedings of the 2025 Conference of the Nations of the Americas Chapter of the Association for Computational Linguistics: Human Language Technologies (Volume 1: Long Papers)*, pp. 11583–11597, 2025.

Zheng, L., Yin, L., Xie, Z., Sun, C. L., Huang, J., Yu, C. H., Cao, S., Kozyrakis, C., Stoica, I., Gonzalez, J. E., et al. Sqlang: Efficient execution of structured language model programs. *Advances in neural information processing systems*, 37:62557–62583, 2024.

Zhong, Y., Liu, S., Chen, J., Hu, J., Zhu, Y., Liu, X., Jin, X., and Zhang, H. {DistServe}: Disaggregating prefill and decoding for goodput-optimized large language model serving. In *18th USENIX Symposium on Operating Systems Design and Implementation (OSDI 24)*, pp. 193–210, 2024.

Appendices

A. Training Details

All training experiments reported in Table 1 were carried out on a single node with 8 A100-SXM4-80G GPUs. For fine-tuning, we used the LMFlow (Diao et al., 2024) framework with three datasets: MetaMathQA-40K (Yu et al., 2023), EvolInstruct-Code-80K (Luo et al., 2023), and xLAM-function-calling-60K (Zhang et al., 2025).

Fine-tuning tasks across all datasets were consistently performed with a batch size of 1, gradient accumulation over 16 steps and a maximum sequence length of 1024 for one epoch. Learning rates were selected via a grid search over $\{1 \times 10^{-4}, 1 \times 10^{-5}, 2 \times 10^{-5}, 5 \times 10^{-5}, 2 \times 10^{-6}, 5 \times 10^{-6}\}$ for each dataset. AdamW (Loshchilov & Hutter, 2017) with $\beta_1 = 0.9$ and $\beta_2 = 0.999$ was used as the optimizer for fine-tuning, together with a weight decay of 0.1 and a warmup ratio of 0.03. There were no explicit regularization setups, including gradient clipping (Pascanu et al., 2013) or dropout (Srivastava et al., 2014).

B. Inference and Serving Details

B.1. Multi-Model Inference Setup and Implementation Details

To ensure a fair comparison with the disaggregated baseline, we fix the input and output token lengths for each model invocation. For the ReAct and Reflexion workloads, we set these lengths based on the token-length statistics reported in prior work (Kim et al., 2025). Once a session is created, it immediately issues the next request upon receiving a model response and continues until all turns in the session complete, without injecting additional delays between model calls. The session arrival rate therefore specifies how frequently new sessions are introduced. Across agent transitions, we apply the same prompt-construction rule—i.e., we incorporate each model’s generated text into the session context in a consistent format—so both PrefillShare and the baseline experience identical context growth and token-length profiles under the same workload.

To rigorously evaluate our method in a realistic multi-agent setting, we developed a proxy-based orchestration layer atop vLLM’s disaggregated serving engine. The system architecture consists of a client-facing proxy, a prefill pool, and a decode pool. Crucially, the prefill pool hosts a single frozen shared base model, while the decode pool consists of multiple workers hosting distinct task-specific fine-tuned models (e.g., Models A, B, C, and D). All implementation details (e.g., routing policy and prefix-cache management) are aligned with the design described in Section 3.3.

The inference workflow is managed by the proxy, which

maintains a routing table mapping a unique User ID to a specific prefill worker to ensure prefix cache locality. When a user initiates a session (e.g., requesting Model A), the proxy routes the prompt to the assigned prefill worker. This worker computes the KV cache using the shared base model and transfers it to the designated decode worker for Model A to generate the response. As the workflow proceeds to the next agent in the chain (e.g., Model B) within the same turn, the proxy routes the request back to the same prefill worker. Since the shared base model already holds the prefix KV cache from the previous invocation, it achieves a cache hit and only computes the KV states for the newly appended tokens. This incrementally updated cache is then transferred to the decode worker for Model B. The same mechanism applies across turns as the session context grows, enabling a single shared prefill module to support heterogeneous fine-tuned models by decoupling prefill computation from model-specific decoding parameters.

B.2. vLLM KV transfer and staging at high concurrency

Our prototype is implemented on top of vLLM’s disaggregated serving pipeline. In the common case, KV caches produced by prefill workers are transferred to decode workers and kept resident in GPU memory, where they are directly consumed during autoregressive decoding.

At high concurrency, when many sessions are concurrently active, the aggregate GPU-resident KV footprint on the decode side can temporarily exceed the available memory capacity. In such cases, vLLM stages a subset of KV caches in CPU memory and reloads them to the GPU when the corresponding sessions are scheduled for decoding. This swap-like staging and reload behavior increases CPU–GPU data movement, which can increase latency and reduce throughput at high concurrency.

We emphasize that this behavior is an implementation-level mechanism in vLLM for handling transient KV memory pressure, rather than an inherent limitation of shared-prefill execution. In principle, alternative designs could mitigate overflow-induced staging via stricter admission control, decode-to-prefill backpressure, or per-session reservation of GPU-resident KV buffers. Exploring such alternatives is orthogonal to PrefillShare and left for future system optimizations.

B.3. Results with a different backbone model

To examine whether the serving behavior observed in Section 4.3 depends on a specific backbone model, we repeat the same experiments using Qwen3-14B in place of LLaMA3.1-8B. All workload configurations, scheduling policies, and evaluation protocols remain identical to those used in the main experiments.

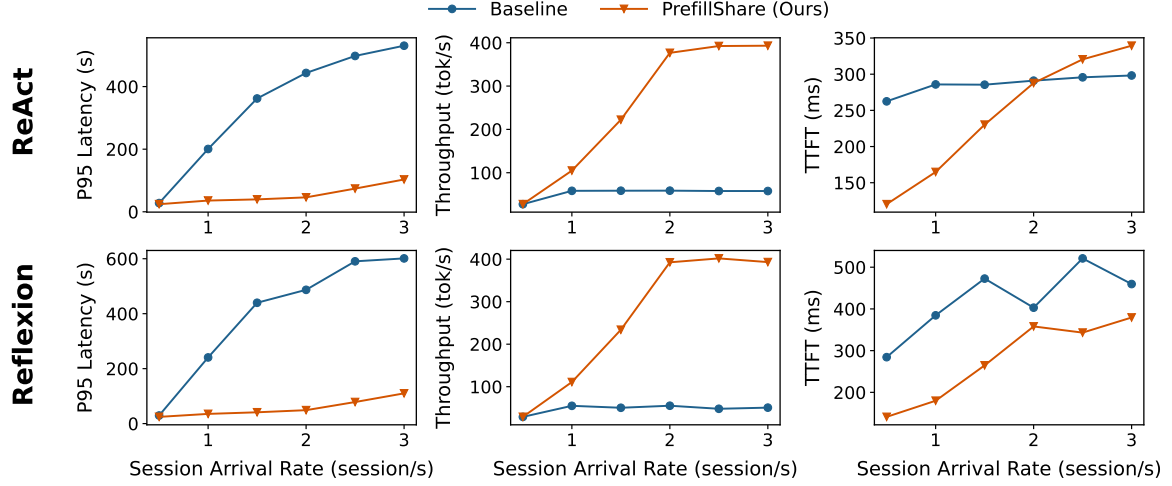


Figure 5. Serving performance under multi-model agent workloads using Qwen3-14B. We replicate the experimental setup of Fig. 3, replacing the LLaMA3.1-8B backbone with Qwen3-14B while keeping all other settings identical. Results are shown for two representative agentic patterns, ReAct (top) and Reflexion (bottom), reporting p95 end-to-end latency, throughput, and TTFT.

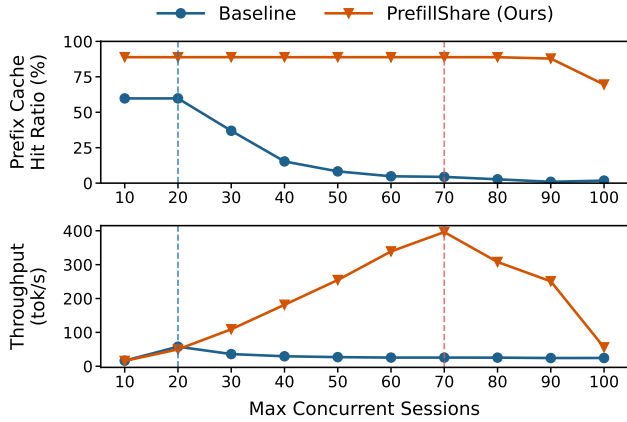


Figure 6. Prefix cache hit ratio and throughput under varying maximum concurrent sessions using Qwen3-14B. This figure mirrors the setup of Fig. 4, with the backbone model replaced by Qwen3-14B. Top: prefix cache hit ratio (%). Bottom: throughput (tok/s).

Fig. 5 reports the serving performance of PrefillShare and the disaggregated baseline under multi-model agent workloads with Qwen3-14B, following the same ReAct and Reflexion patterns as in Fig. 3. Fig. 6 shows the prefix cache hit ratio and throughput as a function of the maximum concurrent sessions, corresponding to the setup of Fig. 4. Across both experiments, PrefillShare continues to achieve substantially higher throughput and lower tail latency than the baseline, while maintaining a high prefix cache hit ratio over a wide concurrency range.

We observe that TTFT trends differ from the main results at higher arrival rates. This difference arises from the operating points selected under our evaluation protocol. As

shown in Fig. 6, PrefillShare reaches its peak throughput at a higher concurrency level than the baseline. At these higher-concurrency operating points, prefill workers experience increased utilization due to more overlapping (partial) prefill operations across in-flight sessions. Since TTFT reflects the latency of the initial prefill stage, increased prefill-side load can lead to higher TTFT even when overall throughput and tail latency improve.